JOC*Article*

A Compact All-Carbon Tripodal Tether Affords High Coverage of Porphyrins on Silicon Surfaces

Kisari Padmaja,[†] Lingyun Wei,[‡] Jonathan S. Lindsey,*[,†] and David F. Bocian*[,‡]

Department of Chemistry, North Carolina State University, Raleigh, North Carolina 27695-8204, and Department of Chemistry, University of California, Riverside, California 92521-0403

jlindsey@ncsu.edu; david.bocian@ucr.edu

Received May 20, 2005

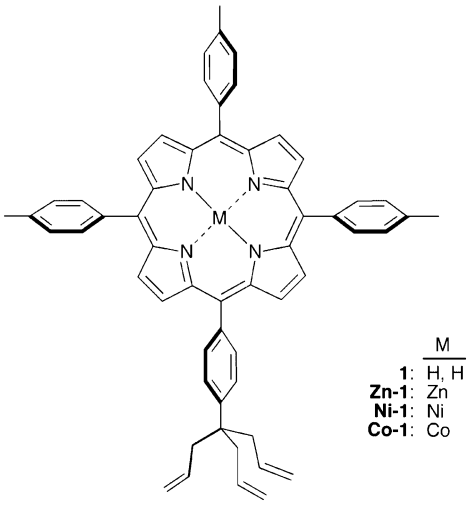

Redox-active molecules designed to give high charge density on electroactive surfaces are essential for applications in molecular information storage. To achieve a small molecular footprint and thereby high surface charge density, a compound consisting of a triallyl tripod attached via a *p*-phenylene unit to a porphyrin (**1**) has been synthesized. The zinc chelate of **1** (**Zn-1**) was attached to Si(100). Electrochemical measurements indicate that the molecular footprint (75 Å) in the monolayer is only ~50% larger than the minimum achievable, indicating high surface coverage. IR spectroscopy indicates that the bands due to the ν(C=C) (1638 cm^{-1}) and γ(CH) (915 cm^{-1}) vibrations present in the solid sample (KBr pellet) are absent from the spectra of the monolayers of **Zn-1**, consistent with saturation of the double bond in each of the three legs of the tripod upon the hydrosilylation process accompanying attachment. Comparison of the relative intensities of the in-plane (998 cm^{-1}) versus out-of-plane (797 cm^{-1}) porphyrin modes indicates the average tilt angle (α) of the porphyrin ring with respect to the surface normal is ~46°, a value also observed for analogous porphyrins tethered to Si(100) via monopodal carbon linkers. Accordingly, the higher packing densities afforded by the compact tripodal linker are not due to a more upright orientation on the surface. The charge-retention half-lives ($t_{1/2}$) for the first oxidation state of the **Zn-1** monolayers increase from 10 to 50 s at low surface coverage ($1-5 \times 10^{-11}$ mol·cm^{-2}) to near 200 s at saturation coverage ($\sim 2 \times 10^{-10}$ mol·cm^{-2}). Taken together, the high surface charge density (despite the lack of upright orientation) of the triallyl-tripodal porphyrin makes this construct a viable candidate for molecular information storage applications.

Introduction

The design and synthesis of redox-active molecules functionalized for surface attachment provides the foundation for information storage devices that operate on the basis of stored charge.[1,2] A key feature of redox-based molecular information storage is that each memory cell

[†] North Carolina State University.
[‡] University of California.

(1) Roth, K. M.; Dontha, N.; Dabke, R. B.; Gryko, D. T.; Clausen, C.; Lindsey, J. S.; Bocian, D. F.; Kuhr, W. G. *J. Vac. Sci. Technol., B* **2000**, *18*, 2359−2364.
(2) Liu, Z.; Yasseri, A. A.; Lindsey, J. S.; Bocian, D. F. *Science* **2003**, *302*, 1543−1545.

10.1021/jo0510078 CCC: $30.25
Published on Web 08/27/2005

CHART 1

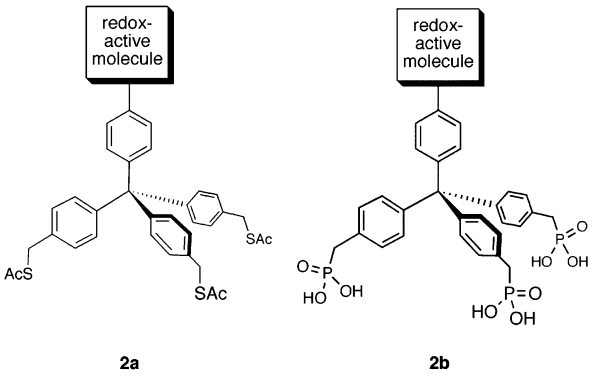

2a **2b**

must store sufficient charge for reliable readout. A requirement for achieving high charge densities is a relatively densely packed monolayer of redox-active molecules. Our previous studies of porphyrinic molecules tethered to both metal and semiconductor surfaces have shown that the maximum achievable surface coverages are in the mid to high 10^{-11} mol·cm^{-2} range, which corresponds to a molecular footprint of 200−300 Å^2.[1−7] This footprint is considerably larger than the 50 Å^2 value we have observed for porphyrins in Langmuir−Blodgett films.[8] If the molecular footprint of the porphyrins on the electroactive surface could be reduced to the value observed for the molecules in Langmuir−Blodgett films, the charge-storage capacity of a memory cell could be increased 4- to 6-fold.

Most of our previous studies of electroactive monolayers utilized molecules that were functionalized for tethering to the surface via a single anchor atom.[1−7] However, we also performed limited studies of molecules functionalized for tethering via multiple anchor atoms, in particular tripodal linkers.[9,10] The rationale for examining the tripods was 2-fold. First, we anticipated that attachment to a surface via three versus one anchor atom might result in a more robust architecture. Second, we thought that the more symmetrical tripodal motif might result in higher packing densities in the monolayers. Two different tripods were examined, each built around a tetraarylmethane unit (Chart 1). For attachment to gold or silicon, the feet of one tripod (**2a**) contained *S*-acetylthiomethyl groups attached to the three aryl units.[10] For attachment to a metal oxide, the feet of the other tripod (**2b**) contained phosphonomethyl groups attached to the three aryl units.[9] The redox-active molecules that were employed with tripod **2a** include a porphyrin, phthalocyanine, ferrocene, ferrocene-porphyrin, and a triple-decker sandwich coordination compound, whereas a zinc porphyrin was incorporated with tripod **2b**. While tripods **2a** and **2b** each represent a satisfactory alternative attachment motif, the studies revealed certain limitations to these linkers: (1) For both tripods **2a** and **2b**, the achievable surface coverages were consistently lower than those for molecules containing single anchor-atom tethers, thereby limiting the charge density of the redox-active monolayer.[9,10] (2) In the case of tripod **2a**, all three sulfur atoms do not in fact bind to the surface, largely compromising the possible advantages of this linker motif (unpublished results). (3) The use of alkylthio groups for attachment to silicon is less attractive than the use of direct alkyl attachment, given the susceptibility of the former to hydrolysis, oxidation, and perhaps reductive displacement.

CHART 2

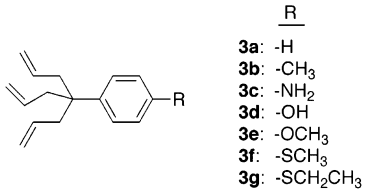

The limitations of tripods **2a** and **2b** prompted us to seek an improved tripod design for linking redox-active molecules to electroactive surfaces. Our initial focus was new tripods for attachment to silicon substrates. In this regard, our previous studies of porphyrin monolayers on silicon revealed that carbon anchors are generally more robust than anchors such as oxygen or sulfur.[6,7] Accordingly, we chose to design the new tripod with alkenyl functionalization to provide attachment via a carbosilane linkage. We also sought a design wherein the tripod is more compact than tripods **2a** and **2b**. We anticipated that this might facilitate attachment to the surface via all three legs of the tripod and potentially to higher packing densities in the monolayers. We ultimately chose a triallyl-substitued arene motif for the tripod. The triallyl-arene compounds (**3a**−**g**) known to date are shown in Chart 2.[12,13] The goal was to extend this chemistry to incorporate the triallyl tripod with a porphyrin unit.

Herein, we first describe the synthesis of the tripodal porphyrins. We then examine the structural and electron-transfer characteristics of one member of this set, the zinc chelate (**Zn-1**), attached to Si(100). The **Zn-1** monolayers on Si(100) were examined using fast-scan cyclic voltammetry to quantitate the packing densities of the monolayers, swept waveform AC voltammetry (SWAV) to elucidate the kinetics of electron transfer,[3] open circuit potential amperometry (OCPA) to determine the time of charge retention after removal of the applied potential,[14]

(3) Roth, K. M.; Gryko, D. T.; Clausen, C.; Li, J.; Lindsey, J. S.; Kuhr, W. G.; Bocian, D. F. *J. Phys. Chem. B* **2002**, *106*, 8639−8648.
(4) Roth, K. M.; Yasseri, A. A.; Liu, Z.; Dabke, R. B.; Malinovskii, V.; Schweikart, K.-H.; Yu, L.; Tiznado, H.; Zaera, F.; Lindsey, J. S.; Kuhr, W. G.; Bocian, D. F. *J. Am. Chem. Soc.* **2003**, *125*, 505−517.
(5) Yasseri, A. A.; Syomin, D.; Malinovskii, V. L.; Loewe, R. S.; Lindsey, J. S.; Zaera, F.; Bocian, D. F. *J. Am. Chem. Soc*. **2004**, *126*, 11944−11953.
(6) Yasseri, A. A.; Syomin, D.; Loewe, R. S.; Lindsey, J. S.; Zaera, F.; Bocian, D. F. *J. Am. Chem. Soc.* **2004**, *126*, 15603−15612.
(7) Wei, L.; Syomin, D.; Loewe, R. S.; Lindsey, J. S.; Zaera, F.; Bocian, D. F. *J. Phys. Chem. B* **2005**, *109*, 6323−6330.
(8) Schick, G. A.; Schreiman, I. C.; Wagner, R. W.; Lindsey, J. S.; Bocian, D. F. *J. Am. Chem. Soc.* **1989**, *111*, 1344−1350.
(9) Loewe, R. S.; Ambroise, A.; Muthukumaran, K.; Padmaja, K.; Lysenko, A. B.; Mathur, G.; Li, Q.; Bocian, D. F.; Misra, V.; Lindsey, J. S. *J. Org. Chem.* **2004**, *69*, 1453−1460.
(10) Wei, L.; Padmaja, K.; Youngblood, W. J.; Lysenko, A. B.; Lindsey, J. S.; Bocian, D. F. *J. Org. Chem.* **2004**, *69*, 1461−1469.
(11) Liu, Z.; Yasseri, A. A.; Loewe, R. S.; Lysenko, A. B.; Malinovskii, V. L.; Zhao, Q.; Surthi, S.; Li, Q.; Misra, V.; Lindsey, J. S.; Bocian, D. F. *J. Org. Chem.* **2004**, *69*, 5568−5577.
(12) Lin, S.-Y.; Hojjat, M.; Strekowski, L. *Synth. Commun.* **1997**, *27*, 1975−1980.
(13) (a) Sartor, V.; Nlate, S.; Fillaut, J.-L.; Djakovitch, L.; Moulines, F.; Marvaud, V.; Neveu, F.; Blais, J.-C.; Létard, J.-F.; Astruc, D. *New J. Chem.* **2000**, *24*, 351−370. (b) Martinez, V.; Blais, J.-C.; Astruc, D. *Org. Lett.* **2002**, *4*, 651−653.
(14) Roth, K. M.; Lindsey, J. S.; Bocian, D. F.; Kuhr, W. G. *Langmuir* **2002**, *18*, 4030−4040.

and Fourier transform infrared (FTIR) spectroscopy to measure the relative orientations of the porphyrin rings with respect to the surface plane.[6,7]

Results and Discussion

Synthesis. Our design of the porphyrin bearing a triallyl tripod incorporates a *p*-phenylene unit between the porphyrin and the central carbon of the tripod. A *p*-tolyl group is present at each of the three nonlinking meso-positions of the porphyrin. The synthesis of the resulting A_3B-porphyrin can be achieved via the condensation of a dipyrromethane-dicarbinol with the dipyrromethane bearing the tripod.[15] The synthesis of the latter begins with commercially available 4-(trifluoromethyl)aniline, which upon reaction with allylmagnesium chloride provides the triallyl-aniline (**3c**)[12] (Scheme 1). The reaction requires 5 equiv of allylmagnesium chloride and involves repetition of fluoride elimination followed by addition of the Grignard reagent to the resulting quinone-imine. The previous synthesis at the 2-mmol scale in diethyl ether afforded **3c** in 54% yield. We carried out the reaction at the 160-mmol scale in THF and obtained **3c** in 87% yield.

The conversion of the triallyl-aniline **3c** to the triallyl-iodobenzene **4** was achieved via the Sandmeyer reaction. Diazotization of amine **3c** in the presence of hydrochloric acid with sodium nitrite at 0−5 °C followed by treatment with potassium iodide gave iodo compound **4** in 28% yield. The Rosenmund−von Braun reaction of **4** with CuCN in DMF afforded the triallyl-cyanobenzene **5** in 89% yield. Reduction of **5** with DIBALH gave the triallyl-benzaldehyde **6** in 91% yield. Treatment of **6** to the standard conditions for dipyrromethane formation (excess pyrrole and $InCl_3$ at room temperature)[16] provided dipyrromethane **7** in 90% yield.

The condensation of the triallyl-dipyrromethane **7** with dipyrromethane-dicarbinol **8-diol** (prepared by reduction of **8** with $NaBH_4$)[17] at room temperature in the presence of a mild Lewis acid $[Yb(OTf)_3]$[18] followed by oxidation with DDQ afforded free base porphyrin **1** in 29% yield. Metalation with $Zn(OAc)_2{\cdot}2H_2O$ at room temperature afforded the desired Zn-porphyrin **Zn-1** in 93% yield. Similar metalation with $Ni(OAc)_2{\cdot}4H_2O$ or $Co(OAc)_2$ provided Ni-porphyrin **Ni-1** or Co-porphyrin **Co-1**, respectively, in high yield (Scheme 2).

Monolayer Characterization. Monolayers of **Zn-1** were prepared on Si(100) substrates and examined via electrochemical and FTIR techniques. The monolayers were prepared on hydrogen-passivated Si(100) surfaces[4] by using a high-temperature (400 °C), 2-min "baking" procedure previously shown to give facile attachment of alkenyl-functionalized porphyrins to Si(100) surfaces.[11] The general electrochemical and vibrational characteristics of the **Zn-1** monolayers are similar to those we have previously reported for other porphyrins tethered to Si(100) via monopodal carbon tethers.[7] Consequently, we will not reiterate these general features herein but rather only describe key features that distinguish the tripodal design from monopodal motifs.

SCHEME 1

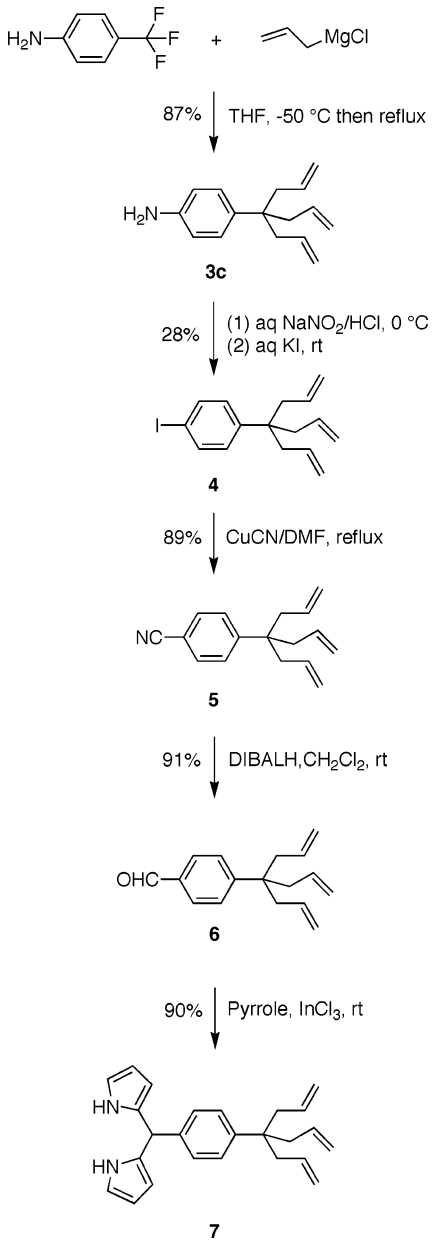

Electrochemical Studies of Surface Coverage, Electron-Transfer Rates, and Charge-Retention Times. The goal of the electrochemical studies was to determine the saturation surface coverage and elucidate the electron-transfer and charge-retention characteristics of the **Zn-1** monolayers. These properties of the monolayers are described below.

A representative fast scan (100 V s^{-1}) cyclic voltammogram for the saturation-coverage **Zn-1** monolayer on a Si(100) microelectrode (100 μm × 100 μm) is shown in Figure 1. At oxidizing potentials, the monolayer exhibits two resolved voltammetric waves indicative of formation of the mono- and dication porphyrin π-radicals. The redox potentials are similar to those observed for this type of porphyrin tethered to Si(100) with other types of linkers.[4,6,7] The surface coverage, Γ, obtained by integrating the voltammetric waves is $\sim 2.2 \times 10^{-10}$ mol·cm^{-2}, a value

(15) Rao, P. D.; Dhanalekshmi, S.; Littler, B. J.; Lindsey, J. S. *J. Org. Chem.* **2000**, *65*, 7323−7344.
(16) Laha, J. K.; Dhanalekshmi, S.; Taniguchi, M.; Ambroise, A.; Lindsey, J. S. *Org. Process Res. Dev.* **2003**, *7*, 799−812.
(17) Tamaru, S.-I.; Yu, L.; Youngblood, W. J.; Muthukumaran, K.; Taniguchi, M.; Lindsey, J. S. *J. Org. Chem*. **2004**, *69*, 765−777.
(18) Geier, G. R., III; Callinan, J. B.; Rao, P. D.; Lindsey, J. S. *J. Porphyrins Phthalocyanines* **2001**, *5*, 810−823.

SCHEME 2

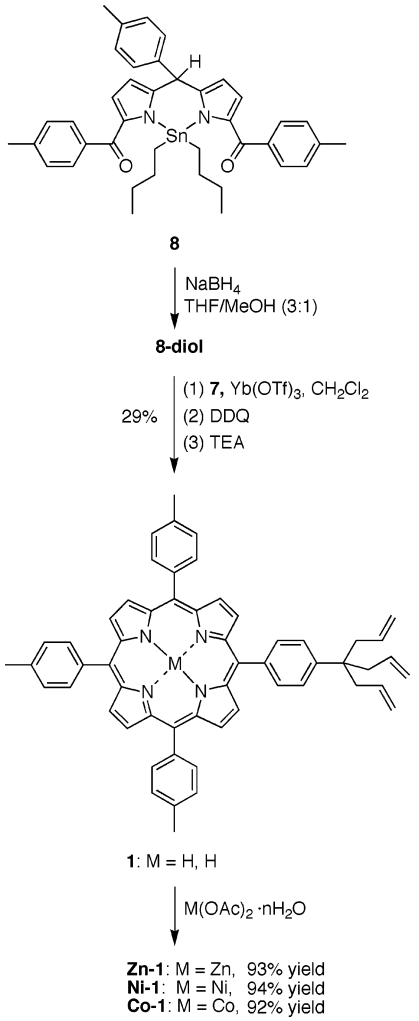

that is approximately 3-fold higher than that obtained for porphyrins with monopodal carbon (oxygen, sulfur, or selenium) tethers. The high saturation coverage observed for the tripodal porphyrin was highly reproducible from electrode to electrode. The surface coverage observed for **Zn-1** corresponds to a molecular footprint of 75 Å^2, a value only 50% larger than that observed for porphyrins in Langmuir−Blodgett films.[8]

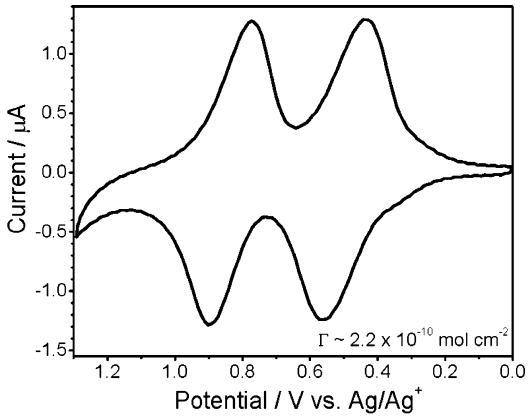

FIGURE 1. Representative fast-scan (100 V s^{-1}) voltammogram of the **Zn-1** monolayers on Si(100).

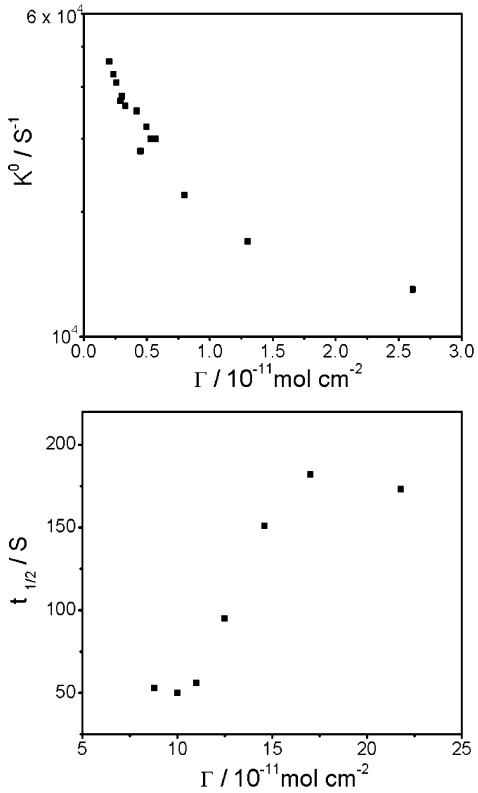

FIGURE 2. Standard electron-transfer rate constants, k^0 (top panel), and charge-retention half-lives, $t_{1/2}$ (bottom panel), versus surface concentration, Γ, for the first oxidation state of the **Zn-1** monolayers on Si(100). Note that the surface concentration ranges shown in the panels are different.

The standard electron-transfer rate constants, k^0, were measured for the first oxidation process ($E^{0/+1}$) of the **Zn-1** monolayers at a variety of coverages from the low 10^{-12} to mid 10^{-11} mol·cm^{-2} range. The interest in this surface-concentration dependence of the electron-transfer rates stems from our previous studies on porphyrin monolayers, both on Si(100) and Au(111), which show that the electron-transfer rates depend on surface coverage.[3,4,6,7,10] As we have previously discussed, the electron-transfer rates cannot be measured at very high surface concentrations, i.e., those near saturation coverages, owing to experimental limitations. Nevertheless, the available concentration range is wide enough to compare the trends observed for the tripodal versus monopodal porphyrins. The electron-transfer rates of **Zn-1** as a function of surface concentration are shown in Figure 2 (top panel). Inspection of these data reveals that the electron-transfer rate decreases with increasing surface concentration, similar to the behavior observed for other types of porphyrin monolayers on both Au(111) and Si(100).[3,4,6,7,10] In addition, the electron-transfer rates observed for **Zn-1** at any particular surface coverage are comparable to those observed for an analogous porphyrin with a monopodal carbon tether.[7]

The charge-retention half-lives, $t_{1/2}$, were also measured at selected surface coverages for the first oxidation state of the **Zn-1** monolayers, in parallel with the studies of the electron-transfer kinetics. Again, the interest in this surface-concentration dependence of charge-retention stems from our previous studies on porphyrin monolayers, both on Si(100) and Au(111), which show that this

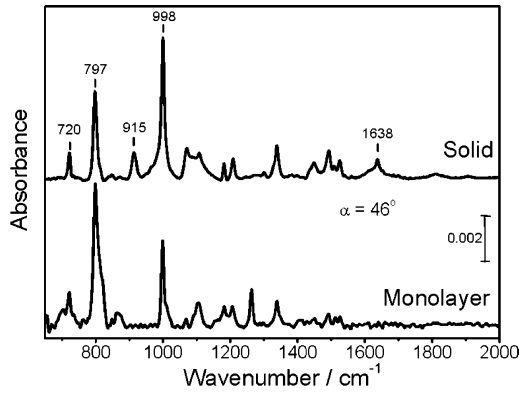

FIGURE 3. FTIR spectra of the solid **Zn-1** porphyrin in a KBr pellet and the corresponding **Zn-1** monolayers on Si(100).

process also depends on surface coverage.[3,4,7,10] We were particularly interested in the charge-retention characteristics of **Zn-1** at high surface coverage, beyond that achievable for porphyrins with monopodal linkers. The charge-retention half-lives of the **Zn-1** monolayers as a function of surface concentration are shown in Figure 2 (bottom panel). Inspection of these data reveals that the charge-retention times for all of the monolayers increase (charge-dissipation rates decrease) as the surface concentration increases, consistent with previous observations on other types of porphyrin monolayers on both Au(111) and Si(100).[3,4,6,10] The charge-retention times for **Zn-1** at surface concentrations in the low to mid 10^{-11} mol·cm^{-2} regime are in the 10−50 s range (data not shown in Figure 2), comparable to that observed for an analogous porphyrin with a monopodal tether.[7] As the surface coverage is increased into the 10^{-10} mol·cm^{-2} range, the charge-retention times increase, peaking near 200 s at saturation coverage.

FTIR Studies of Adsorption Geometry. The electrochemical studies show that the tripodal linker affords significantly higher surface coverage than either tripod **2a** and **2b** or any of the types of monopodal linkers we have previously examined. The higher surface coverage afforded by the compact tripod versus the previous more bulky designs is easily rationalized, given the limitations of the latter linkers. On the other hand, the higher coverage of the compact tripod versus the monopodal linkers is less obvious. In this regard, our previous studies of porphyrins attached to Au(111) and Si(100) via monopodal tethers have shown that the molecules are significantly tilted with respect to the surface normal.[5−7] Accordingly, one possible explanation for the higher packing densities exhibited by the compact tripod is that this design leads to a more upright orientation for the porphyrin. To explore this issue, we probed the adsorption geometry of the porphyrin using FTIR spectroscopy.

The mid-frequency (700−1900 cm^{-1}) IR spectrum of the saturation-coverage **Zn-1** monolayer is shown in the bottom trace of Figure 3; the spectrum of a solid sample of the parent porphyrin is shown in the top trace for comparison. The IR spectra of the tripodal porphyrin in both the monolayer and solid forms are similar to those we have previously reported for an analogous porphyrin with a monopodal linker.[7] The key vibrational signatures relevant to our studies are the porphyrin pyrrole in-plane ring breathing mode near 998 cm^{-1},[19] and the out-of-plane β-pyrrole hydrogen deformation at 797 cm^{-1}.[20] For the solid sample, other important features are the C=C stretching vibration, ν(C=C), of the alkene group in the linker at 1638 cm^{-1} and out-of-plane C−H deformation, γ(CH), of this group at 915 cm^{-1}.[21] [Note that only weak bands are seen in the high-frequency (2600−3400 cm^{-1}) spectral region (not shown), all attributable to C−H stretches.]

Comparison of the IR spectra of the solid and monolayers reveals that the bands due to the ν(C=C) (1638 cm^{-1}) and γ(CH) (915 cm^{-1}) vibrations are absent from the spectra of the monolayers. The absence of these bands is consistent with saturation of the double bond in each of the three legs of the tripod. These data are consistent with, although not definitive proof of, the view that each of the three legs of the compact tripod attaches to the Si(100) surface via a hydrosilylation reaction (as expected when an alkene reacts with hydrogen-passivated silicon[22]).

The relative intensities of the in-plane (998 cm^{-1}) versus out-of-plane (797 cm^{-1}) porphyrin modes can be used to determine the average tilt angle (α) of the porphyrin ring with respect to the surface normal.[23] The average angle determined for the porphyrins in the **Zn-1** monolayers is ∼46,° a value that is generally similar to those we have observed for analogous porphyrins tethered to Si(100) via monopodal carbon linkers.[7] Accordingly, the higher packing densities afforded by the compact tripodal linker are not due to a more upright orientation on the surface.

Conclusions

The motivation for preparing the porphyrin bearing a compact tripodal tether was to achieve an upright orientation and therefore a small molecular footprint on an electroactive surface. The resulting high surface coverage would afford a high charge density for molecular information storage applications. The studies reported herein demonstrate that the tripodal porphyrin does indeed afford a reasonably small footprint (within ∼50% of the minimum expected), but surprisingly, the molecules are not organized in an upright fashion. The ability of the tripodal porphyrin to achieve a higher packing density than a monopodal-functionalized porphyrin may arise because of torsional constraints at the carbon-atom junction of the three alkyl legs and the phenylene linker to the porphyrin. These constraints would restrict motion along the full length of the lever arm that links the porphyrin to the surface. We also note that tilting is not generally inconsistent with a small molecular footprint. In particular, the porphyrins in the very densely packed Langmuir−Blodgett films are significantly tilted with

(19) Li, X. Y.; Czernuszewicz, R. S.; Kincaid, J. R.; Su, Y. O.; Spiro, T. G. *J. Phys. Chem.* **1990**, *94*, 31−47.
(20) Li, X. Y.; Czernuszewicz, R. S.; Kincaid, J. R.; Spiro, T. G. *J. Am. Chem. Soc.* **1989**, *111*, 7012−7023.
(21) Silverstein, R. M.; Bassler, G. C. *Spectrophotometric Identification of Organic Compounds*; Wiley: New York, 1967.
(22) (a) Buriak, J. M. *Chem. Commun*. **1999**, 1051−1060. (b) Buriak, J. M. *Chem. Rev*. **2002**, *102*, 1271−1308.
(23) (a) Painter, P. C.; Coleman, M. M.; Koenig, J. L. *The Theory of Vibrational Spectroscopy and Its Application to Polymeric Materials*; Wiley: New York, 1982. (b) Allara, D. L.; Nuzzo, R. G. *Langmuir* **1985**, *1*, 52−66. (c) Harrick, N. J.; Mirabella, F. M. *International Reflection Spectroscopy: Review and Supplement*; Harrick Scientific Corp.: New York, 1985. (c) Greenler, R. G. *J. Chem. Phys.* **1966**, *44*, 310−315. (d) Zaera, F. *Int. Rev. Phys. Chem.* **2002**, *21*, 433−471.

respect to the surface normal.[8] Finally, we note that attachment via three legs of the compact tripod and a tilted orientation for the porphyrin are not inconsistent. Molecular models of the tripod on the Si(100) surface show that tilted orientations are possible owing to the torsional flexibility of the alkane chains in the linker. Regardless of the origin of the increased packing density afforded by the compact tripod, this adsorption characteristic has important consequences for molecular information storage in that higher surface coverage results in longer charge-retention times.

Experimental Section

Synthesis. 5-[4-(4-Allylhepta-1,6-dien-4-yl)phenyl]-10,15,20-tri-*p*-tolylporphyrin (1). Following a general procedure,[17,18] a solution of **8**[17] (0.42 g, 0.60 mmol) in THF/MeOH (10:1, 24 mL) was treated with $NaBH_4$ (0.91 g, 24 mmol) at room temperature. After 2 h, the reaction mixture was quenched with saturated aqueous NH_4Cl and extracted with CH_2Cl_2. The organic phase was dried (Na_2SO_4) and concentrated to provide the corresponding dicarbinol **8-diol**. The resulting dicarbinol was then immediately subjected to condensation with dipyrromethane **7** (214 mg, 0.600 mmol) in the presence of $Yb(OTf)_3$ (2.98 g, 4.81 mmol) in CH_2Cl_2 (240 mL). After 80 min, DDQ (409 mg, 1.80 mmol) was added and the mixture was stirred for 1 h. Then TEA (2.40 mL) was added and the mixture was stirred for about 30 min. The reaction mixture was passed through a pad of silica and eluted with CH_2Cl_2. The porphyrin band was collected and chromatographed [silica, hexanes/ethyl acetate (9:1 → 4:1)] to provide a pink solid (139 mg, 29%): ^{1}H NMR δ −2.75 (s, 2H), 2.65−2.74 (m, 15H), 5.12−5.24 (m, 6H), 5.77−5.93 (m, 3H), 7.46−7.60 (m, 6H), 7.65 (d, J = 8.0 Hz, 2H), 8.04−8.12 (m, 6H), 8.14 (d, J = 8.0 Hz, 2H), 8.76−8.83 (m, 2H), 8.83−8.92 (m, 6H); MALDI-MS obsd 791.1; FABMS obsd 791.4146, calcd 791.4114 [$(M + H)^+$, M = $C_{57}H_{50}N_4$]; λ_{abs} 421, 516, 551, 594, 649 nm.

Zinc(II)-5-[4-(4-allylhepta-1,6-dien-4-yl)phenyl]-10,15,20-tri-*p*-tolylporphyrin (Zn-1). A solution of **1** (131.8 mg, 167 μmol) in $CHCl_3$ (13 mL) was treated with a solution of $Zn(OAc)_2 \cdot 2H_2O$ (183 mg, 0.832 mmol) in MeOH (2.6 mL) at room temperature. The reaction was followed by TLC. The reaction was complete in 2 h. The reaction mixture was washed with saturated aqueous NH_4Cl and extracted with CH_2Cl_2. The combined organic layer was dried (Na_2SO_4), concentrated, and chromatographed [silica, hexanes/ethyl acetate (9:1)] to afford a pink solid (132 mg, 93%): ^{1}H NMR δ 2.66−2.78 (m, 15H), 5.12−5.28 (m, 6H), 5.80−5.96 (m, 3H), 7.50−7.60 (m, 6H), 7.67 (d, J = 8.4 Hz, 2H), 8.04−8.14 (m, 6H), 8.16 (d, J = 8.4 Hz, 2H), 8.88−8.94 (m, 2H), 8.94−9.02 (m, 6H); MALDI-MS obsd 852.4; FABMS obsd 852.3193, calcd 852.3170 ($C_{57}H_{48}N_4Zn$); λ_{abs} 424, 551 nm.

Nickel(II)-5-[4-(4-allylhepta-1,6-dien-4-yl)phenyl]-10,15,20-tri-*p*-tolylporphyrin (Ni-1). A solution of **1** (12.3 mg, 15 μmol) in $CHCl_3$ (1.9 mL) was treated with a solution of $Ni(OAc)_2 \cdot 4H_2O$ (3.8 mg, 15 μmol) in MeOH (0.5 mL) at room temperature. The reaction was followed by TLC. The reaction did not proceed even after 9 h. Therefore, an additional portion of $Ni(OAc)_2 \cdot 4H_2O$ (85 mg, 0.34 mmol) in MeOH (4 mL) and $CHCl_3$ (16 mL) was added, and the reaction mixture was refluxed. After 11 h, some free base porphyrin remained. Another portion of $Ni(OAc)_2 \cdot 4H_2O$ (8.0 mg, 32 μmol) in MeOH (1 mL) was added and the reaction mixture was allowed to reflux for another 2 h. The reaction mixture was concentrated and then CH_2Cl_2 was added. The organic solution was washed with water, dried (Na_2SO_4), concentrated, and chromatographed [silica, hexanes/CH_2Cl_2 (2:1)] to afford a pink solid (12 mg, 94%): ^{1}H NMR δ 2.60−2.71 (m, 15H), 5.08−5.22 (m, 6H), 5.72−5.90 (m, 3H), 7.42−7.52 (m, 6H), 7.60 (d, J = 8.4 Hz, 2H), 7.84−7.92 (m, 6H), 7.95 (d, J = 8.4 Hz, 2H), 8.66−8.82 (m, 8H); MALDI-MS obsd 847.2; FABMS obsd 846.3284, calcd 846.3232 ($C_{57}H_{48}N_4Ni$); λ_{abs} 417, 528 nm.

Cobalt(II)-5-[4-(4-allylhepta-1,6-dien-4-yl)phenyl]-10,15,20-tri-*p*-tolylporphyrin (Co-1). A solution of **1** (13.9 mg, 18 μmol) in $CHCl_3$ (8.5 mL) was treated with a solution of $Co(OAc)_2$ (31.1 mg, 176 μmol) in MeOH (1.7 mL) at room temperature. The reaction mixture was refluxed for 8 h with monitoring by TLC. The reaction mixture was concentrated and then CH_2Cl_2 was added. The organic solution was washed with water, dried (Na_2SO_4), concentrated, and chromatographed [silica, hexanes/CH_2Cl_2 (2:1)] to afford a red solid (14 mg, 92%): ^{1}H NMR δ 3.80−3.98 (m, 6H), 4.08−4.26 (br, 9H), 6.00−6.20 (m, 6H), 7.10−7.23 (br, 3H), 9.65−9.95 (m, 8H), 12.6−13.6 (br, 8H), 15.60−16.60 (br, 8H); MALDI-MS obsd 848.1; FABMS obsd 847.3267, calcd 847.3211 ($C_{57}H_{48}CoN_4$); λ_{abs} 413, 530 nm.

4-(4-Allylhepta-1,6-dien-4-yl)aniline (3c). Following a literature procedure carried out at the 2-mmol scale,[12] a 2 M solution of allylmagnesium chloride in THF (0.400 L, 0.800 mol) was diluted with additional THF (1.00 L) and then treated dropwise with a solution of 4-(trifluoromethyl)aniline (19.9 mL, 0.160 mol) in THF (210 mL) at −50 °C under argon. After complete addition the sides of the reaction flask were rinsed with additional THF (150 mL). The resulting mixture was heated at reflux. The reaction was monitored by TLC for the complete consumption of 4-(trifluoromethyl)aniline. After 3.5 h, the mixture was concentrated and then CH_2Cl_2 was added. The organic solution was washed with water, dried (Na_2SO_4), and filtered. The filtrate was concentrated and chromatographed [silica, CH_2Cl_2/hexanes (2:1)], affording a pale yellow solid (31.7 g, 87%): ^{1}H NMR δ 2.36−2.43 (m, 6H), 3.48−3.66 (br, 2H), 4.94−5.06 (m, 6H), 5.50−5.64 (m, 3H), 6.62−6.70 (m, 2H), 7.06−7.12 (m, 2H); ^{13}C NMR δ 42.1, 42.6, 115.0, 117.5, 127.6, 135.0, 135.8, 144.1; FABMS obsd 228.1757, calcd 228.1752 [$(M + H)^+$, M = $C_{16}H_{21}N$].

1-(4-Allylhepta-1,6-dien-4-yl)-4-iodobenzene (4). A solution of concentrated HCl/H_2O (1:1 v/v, 44 mL) was added to a solution of **3c** (11.4 g, 50.2 mmol) in THF (80 mL). The mixture was stirred at room temperature for 75 min and then cooled to 0−5 °C. A chilled solution of $NaNO_2$ (7.99 g, 116 mmol) in water (80 mL) was added while maintaining the temperature of the reaction mixture below 5 °C. Additional H_2O (30 mL) was added. The reaction mixture was tested for the presence of nitrous acid with KI-starch paper. A solution of KI (14.2 g, 85.5 mmol) in H_2O (16 mL) cooled to ∼5 °C was added, again maintaining the mixture at <5 °C throughout the addition. Additional H_2O (24 mL) and THF (150 mL) were added. The reaction mixture was then gradually allowed to warm to room temperature. After ∼6.5 h, the reaction mixture was neutralized with saturated aqueous Na_2CO_3 and then filtered. The filtrate was concentrated. The resulting residue was dissolved in CH_2Cl_2 and washed with water. The organic phase was dried (Na_2SO_4), concentrated, and chromatographed (silica, hexanes) to afford a colorless liquid (4.73 g, 28%): ^{1}H NMR (300 MHz) δ 2.38−2.50 (m, 6H), 4.94−5.12 (m, 6H), 5.44−5.64 (m, 3H), 7.00−7.12 (m, 2H), 7.58−7.70 (m, 2H); ^{13}C NMR δ 41.8, 42.0, 43.5, 91.4, 117.8, 118.2, 129.1, 134.2, 137.3, 145.8.

4-(4-Allylhepta-1,6-dien-4-yl)benzonitrile (5). Following a literature procedure,[24] a mixture of **4** (5.07 g, 15.0 mmol), CuCN (2.03 g, 22.6 mmol) and DMF (50 mL) was heated over the course of 30 min until refluxing was attained. The mixture was refluxed for 3 h. The reaction was monitored by TLC. The mixture was poured into a flask containing crushed ice and concentrated aqueous NH_4OH (200 mL). The resulting mixture was bubbled with oxygen for 14 h. The resulting dark blue mixture was then filtered. The layers of the filtrate were separated, and the aqueous layer was extracted with CH_2Cl_2. The combined organic layer was dried (Na_2SO_4), concentrated, and chromatographed [silica, hexanes/ethyl acetate (19:1)] to afford a colorless liquid (3.17 g, 89%): IR (CH_2Cl_2) 2230 cm^{-1}; ^{1}H NMR (300 MHz) δ 2.40−2.54 (m, 6H), 4.94−5.12 (m, 6H),

(24) Hanack, M.; Haisch, P.; Lehmann, H.; Subramanian, L. R. *Synthesis* **1993**, 387−390.

5.40−5.62 (m, 3H), 7.36−7.48 (m, 2H), 7.56−7.68 (m, 2H); ^{13}C NMR δ 41.6, 44.2, 109.8, 118.6, 119.1, 127.8, 132.0, 133.5, 151.7; FABMS obsd 238.1589, calcd 238.1596 [$(M + H)^+$, M = $C_{17}H_{19}N$].

4-(4-Allylhepta-1,6-dien-4-yl)benzaldehyde (6). Following a literature procedure,[25] a solution of **5** (2.21 g, 9.32 mmol) in CH_2Cl_2 (25 mL) was cooled to 0 °C and was treated dropwise with a 1 M solution of DIBALH in hexanes (11.2 mL, 11.2 mmol). The mixture was allowed to slowly warm to room temperature. The reaction was monitored by TLC. After 3 h, the reaction mixture was poured into a beaker containing crushed ice and 6 N HCl. The mixture was stirred for about 1 h. The layers were separated and the aqueous phase was extracted with CH_2Cl_2. The combined organic layer was washed with aqueous $NaHCO_3$ followed by water. The organic layer was dried (Na_2SO_4), concentrated, and chromatographed [silica, hexanes/ethyl acetate (19:1)] to afford a colorless liquid (2.04 g, 91%): IR (CH_2Cl_2) 3078, 1705 cm^{-1}; ^{1}H NMR (300 MHz) δ 2.44−2.59 (m, 6H), 4.94−5.14 (m, 6H), 5.44−5.66 (m, 3H), 7.45−7.58 (m, 2H), 7.80−7.93 (m, 2H), 9.99 (s, 1H); ^{13}C NMR δ 41.8, 44.3, 118.4, 127.6, 129.6, 133.8, 134.4, 153.4, 192.0; FABMS obsd 241.1597, calcd 241.1592 [$(M + H)^+$, M = $C_{17}H_{20}O$].

5-[4-(4-Allylhepta-1,6-dien-4-yl)phenyl]dipyrromethane (7). Following a general procedure,[16] a degassed solution of **6** (1.54 g, 6.42 mmol) in pyrrole (45 mL, 649 mmol) at room temperature was treated with $InCl_3$ (136 mg, 0.615 mmol). The mixture was stirred for 4 h, during which the mixture turned greenish brown. The reaction was quenched by the addition of NaOH (769 mg, 19.2 mmol, 20−40 mesh beads). The reaction mixture was stirred for 1 h and then filtered through a plug of cotton. The filtered material was washed with CH_2Cl_2. The filtrate was concentrated and then diluted with CH_2Cl_2. The organic solution was washed with water, then dried (Na_2SO_4), concentrated, and chromatographed [silica, hexanes/ethyl acetate (4:1)] to provide a dark brown viscous liquid (2.05 g, 90%): ^{1}H NMR δ 2.38−2.48 (m, 6H), 4.96−5.02 (m, 4H), 5.02−5.05 (m, 2H), 5.42 (s, 1H), 5.48−5.61 (m, 3H), 5.86−5.90 (m, 2H), 6.13−6.17 (m, 2H), 6.64−6.68 (m, 2H), 7.08−7.18 (m, 2H), 7.23−7.28 (m, 2H), 7.85 (br, 2H); ^{13}C NMR δ 42.1, 43.3, 43.7, 107.4, 108.6, 117.4, 117.8, 127.2, 128.2, 132.9, 134.7, 139.5, 144.7. FABMS obsd 356.2256, calcd 356.2252 ($C_{25}H_{28}N_2$).

Monolayer Preparation and Characterization. Electrode Preparation. The electrochemical measurements on the monolayers were made using highly doped *p*-type Si(100) working microelectrodes (100 μm × 100 μm) prepared via photolithographic methods as described previously.[4] A microelectrode was used to ensure that the RC time constant of the electrochemical cell was sufficiently short so that the electron-transfer kinetics of the porphyrin monolayers could be measured accurately.

A bare Ag wire was used as the counter/reference electrode. The electrode was prepared by sonicating a section of 500 μm diameter Ag wire in 7.0 M NH_4OH, rinsing it in deionized water and ethanol, then sonicating it in CH_2Cl_2 containing 1.0 M *n*-Bu_4NPF_6. The Ag wire prepared in this manner was placed inside a 10 μL polypropylene pipet tip containing ∼5 μL of the propylene carbonate/1.0 M *n*-Bu_4NPF_6 electrolyte solution and manipulated using a micropositioning device in a setup previously described.[4]

Monolayer Preparation. All of the monolayers were assembled on hydrogen-passivated Si(100) surfaces, prepared as described previously,[4] by using a high-temperature (400 °C), short-time (2 min) "baking" attachment procedure previously shown to give facile attachment of alkenyl-functionalized porphyrins to Si(100) surfaces.[11] The surface coverage and conditions for achieving saturation coverage were determined electrochemically in a series of experiments wherein the concentration of the porphyrin in the deposition solution (benzonitrile) was varied systematically. These experiments revealed that the surface coverage could be varied in a controlled fashion from the low 10^{-12} mol·cm^{-2} to the low 10^{-10} mol cm^{-2} range (saturation coverage) by varying the porphyrin concentration from ∼2 μM to ∼2 mM.

The monolayers for the electrochemical experiments were prepared by dispensing a 2 μL drop of the porphyrin solution onto the surface of the microelectrode contained in a sparged VOC vial sealed under Ar. The monolayers prepared for the FTIR experiments utilized much larger platforms (∼1 cm^2), and consequently required a larger drop size, ∼50 μL. After deposition, the vial containing the Si substrate was heated on a hotplate at 400 °C for 2 min and then removed and purged with Ar until cooling to room temperature. Finally, the Si substrate was rinsed and sonicated five times with anhydrous CH_2Cl_2 and purged dry once again under Ar.

Electrochemical Measurements. The electrochemical measurements on **Zn-1** in solution were made in a standard three-electrode cell using Pt working and counter electrodes and a Ag/Ag^+ reference electrode. The solvent/electrolyte was CH_2Cl_2 containing 0.1 M Bu_4NPF_6. The electrochemical measurements on the **Zn-1** monolayers were performed in a two-electrode configuration using the fabricated Si(100) microelectrode and a Ag counter/reference electrode previously described,[4] and propylene carbonate containing 1.0 M Bu_4NPF_6 as the solvent/electrolyte. The RC time constant for this microelectrode/electrochemical cell, measured to be ∼4 μs, is sufficiently short to preclude any significant interference with the measurement of the electron-transfer rates. The cyclic voltammograms were recorded using a Gamry Instruments PC4-FAS1 femtostat running PHE 200 Framework and Echem Analyst software. The surface coverage of the porphyrins in the monolayer was determined by integration of the total charge in the first anodic wave and by using the geometric dimensions of the microelectrode. The standard electron-transfer rate constants, k^0, of the porphyrin monolayers were obtained using the same SWAV method previously used to obtain k^0 values for porphyrin monolayers on both Au and Si surfaces.[3−6] The rates of charge dissipation after disconnection from the applied potential, reported as charge-retention half-lives, $t_{1/2}$, were obtained using the OCPA method also used previously to obtain $t_{1/2}$ values for porphyrin monolayers on both Au and Si surfaces.[4,7,14]

FTIR Spectroscopy. The FTIR spectra of the **Zn-1** porphyrin in both solid and monolayer forms were collected at room temperature with a spectral resolution of 4 cm^{-1}. The spectra of solid **Zn-1** porphyrin were obtained in KBr pellets (ca. 1−2 wt % porphyrin). These spectra were collected in transmission mode using a room-temperature DTGS detector by averaging over 32 scans.

The IR spectra of the **Zn-1** monolayers were obtained using a Harrick Scientific horizontal reflection Ge attenuated total reflection accessory (GATR, 65° incidence angle). The Si substrates were placed in contact with the flat surface of a semispherical Ge crystal that serves as the optical element, and IR spectra were collected with p polarized light using a liquid-nitrogen cooled medium-bandwidth (600−4000 cm^{-1}) MCT detector and averaging over 256 scans. The spectra of the porphyrin monolayers were referenced against that of a hydrogen-terminated Si(100) surface previously subjected to the same deposition conditions as those used to obtain the monolayer but using only the neat deposition solvent. The Ge crystal was cleaned with neat 2-butanone before every experiment, and the GATR accessory was purged with dry N_2 during data acquisition.

Acknowledgment. This work was supported by the Center for Nanoscience Innovation for Defense and DARPA/DMEA (award H94003-04-2-0404) and by ZettaCore, Inc.

Supporting Information Available: General experimental section and spectral data for selected compounds. This material is available free of charge via the Internet at http://pubs.acs.org.

JO0510078

(25) Lindsey J. S.; Prathapan, S.; Johnson, T. E.; Wagner, R. W. *Tetrahedron* **1994**, *50*, 8941−8968.